Journal of Harbin Engineering University Vol 44 No. 7
ISSN: 1006-7043 July 2023

Predicting Liver Cancer Patients on Covid-19 Pandemic Using Deep Learning (DL) Method

K.C. Chandra Sekaran
Associate Professor, Department of Computer Science, Alagappa Govt. Arts College,
Karaikudi, Tamilnadu, India.
Mail: chandrasekarankc@agacollege.in
K. Radha Krishnan
Assistant Professor, Department of Computer Science, Dr. Ambedkar Govt. Arts College,
Vyasarpadi, Chennai, Tamilnadu,
Mail: radhakrishnan.2018123@gmail.com

Abstract: Liver cancer (LC) is one of the most rapidly growing types of cancer worldwide. Lower death rates result from the early identification of liver cancer. Due to COVID-19's high infectiousness, a large influx of patients can enter hospitals at once for both detection and treatment, which posed a significant challenge to the nation's public healthcare institutions. The COVID-19 epidemic has adversely impacted cancer patients. The COVID19 pandemic's negative effects on cancer patients who contract the virus, its effects on the accessibility of cancer treatment, and the significant interruption to cancer research are only a few examples of this effect. The population of cancer patients is diverse, and current research has now identified characteristics that enable risk categorization of cancer patients in order to improve therapy. The severity of the symptoms based on initial assessment frequently determines the priority of the treatment. Clinically, it has been difficult to predict outcomes for patients with liver cancer having COVID-19. The severity of the disease has been retrospectively linked to a large number of clinical characteristics, but it is still unclear how well these variables predict disease progression or how many variables interact to enhance risk. This research focuses on sequential analysis to extract features using activation function in the Long Short Term Memory (LSTM) as Deep Learning (DL) techniques. The COVID-19 effect on Liver Cancer Prediction dataset is used to predict LC during COVID-19 impact. Additionally, the findings of this experiment demonstrated that DL models performed better in terms of accuracy with leaky relu activation function classifier than other activation function classifiers.

Keywords: Liver Cancer, COVID-19 Data, Deep Learning Methods, Long Short Term Memory (LSTM) classifier.

1. Introduction

The most common type of cancer is LC, which has the highest death rate. Over 700,000 people worldwide are diagnosed with cancer each year [1]. The sixth most prevalent type of cancer worldwide is liver cancer. Every year, more than 600,000 people die as a result of liver cancer. The disease is predicted using the symptoms identified in clinical studies. If a liver disease is predicted, the patient is advised to have a Liver Function Test (LFT) [2]. Humans' livers are a large, granular organ. The rise in acute liver disease, cirrhosis and chronic liver disease is directly related to lifestyle changes. The LC has evolved into the most common type of the disease in many areas as a result of the above-mentioned issues [3]. Early cancer detection opens up a wider range of therapeutic options. While a physical examination is not feasible, the only way to diagnose liver cancer via imaging or radiology tests. With the help of imagination testing, cancer can be detected early and the effectiveness of post-treatment care can be evaluated [4].

The LC has posed a severe threat to human life in recent years, as both its morbidity and fatality rates have increased globally. Low predictability, quick decline, and an easier mortality following malignancy are the primary clinical characteristics of liver cancer. The identification of liver cancer is crucial since early detection is the key to successful treatment [5-7]. Imaging diagnosis, Serum tests and biopsies are currently the three

main ways to diagnose liver cancer. The histopathological pictures of LC can clearly show the satellite foci and metastases, lesions of the liver tissue surrounding the disease, and their location, size, quantity, level of differentiation, cell and histological type, vascular and capsular invasion. The level of distinction between them may indicate the severity of the cancer. The level of malignancy decreases with increasing differentiation and proximity to normal tissue cells. The degree of malignancy increases as differentiation decreases. The identification and management of various degrees of differentiation are essential for patient survival rates and survival times [8, 9]. In order to diagnose liver cancer with various levels of differentiation, precise classification of histological images of the disease is essential and indispensable.

The beta-coronavirus that causes Severe Acute Respiratory Syndrome (SARS-CoV-2) is the source of the infectious disease known as coronavirus disease-2019 (COVID-19), which has spread quickly and to the point of pandemic proportions around the world. Liver Disease Associated to Metabolic Dysfunction (MAFLD) has recently replaced Non-Alcoholic Fatty Liver Disease (NAFLD) as the term for the relationship between hepatic steatosis, diabetes, obesity/overweight and metabolic dysregulation [10]. There are currently very few published data on the incidence of liver disease specifically MAFLD among COVID-19 individuals. However, metabolic patients particularly those in their initial years, who have a fatty liver and hepatic involvement appear to be at a greater chance for severe COVID-19 symptoms [11, 12]. It has been suggested that this association between the severity of respiratory symptoms and MAFLD may be clarified by the fact that patients with metabolic-associated hepatic steatosis or steatohepatitis have higher expression levels of the cellular serine protease TMPRSS2 (ACE2/TMPRSS2) and the angiotensin-converting enzyme 2 receptors, which are both used by SARS-CoV-2 and could promote the penetration of the pathogenic virus into cells. It should be noted that Meijnikman et al.'s study relies on RNA transcriptomic analysis rather than measurement of protein levels or ACE2 activity [13].

The COVID-19 pandemic caused clinical practices at over 87% of the centers (n = 66), with nearly half (48%) reducing on number of doctors assigned to treating LC patients. The main modifications to the clinical practice are shown in Figure 1: The screening programme was adjusted by 80.9%, LC patient's the imaging follow-up was changed by 73.5%, locoregional therapies were changed by 52.9% and surgical treatments were postponed by 63.2%. The percentage of regions where clinical practices were changed based on continent is shown in Figures S1 and S2. 21.1% of centers (n = 16/76) tested for SARS-CoV-2 infection prior to an outpatient consultation for LC management, and 76.3% of centers (n = 58/76) tested prior to any predetermined admission of patients for LC therapy [14].

Algorithms based on artificial intelligence have become increasingly prevalent in the medical industry in recent years due to the field's rapid progress. The ML technique known as "deep learning" is based on deep neural networks that is one of the artificial intelligence algorithms [15]. Natural language processing and computer vision tasks both frequently use deep learning. Hence, the accurate prediction perform using DL for liver cancer patients with COVID-19 is essential in the current situation to avoid mortality. Thus, the research focuses on effective sequential pattern with LSTM technique for providing high accuracy in accomplishing detection of LC even during COVID-19 patients.

The organisation of paper is structured are as follow, the session 2 discusses the automatic feature extraction through classification using DL methods. The session 3 discuss the architecture of LSTM with activation function through sequential pattern in the LC during COVID-19. The session 4 discusses performance analysis of LSTM with various activation function through confusion matrix metrics. Session 5 conclude that leaky relu as activation function on LSTM model has performed high accuracy in diagnosing the LC precisely at COVID-19 pandemic situation.

2. Literature Review

The most critical situation faced by the healthcare is about diagnosing the LC during pandemic situation. The literature has supported in

identifying the standard procedure as well as the automatic computing for diagnosing LC through various ML and DL technique which are discussed as follows. Lin et al. has recently employed multiphoton imaging and deep learning to automatically classify the differentiation of HCC [16]. In order to fulfil the necessity of completing difficult visual identification tasks, such as classifying tumor subtypes and differentiating tumors from healthy tissue samples, more complex neural networks may now be trained thanks to the advancement of visual processing units [17]. On histopathology pictures, Coudray et al. used a deep convolutional neural network to classify lung tumor types and subtypes automatically. A favorable outcome was also obtained for the categorization of colorectal cancer with deep learning technique [18]. In order to help pathologists for accurately identify gene alterations and cancer subtypes, deep-learning algorithms may be deployed. Deep learning's applicability to solid tumors, notably HCC, is still up for debate. The need for predictive assays in frozen slides that allow for the identification and categorization of patients for extra therapy during surgery has also increased as a result of advancements in AI technologies in digital pathology [19].

Ashreetha, B. advises utilizing Gabor Features (GF) in conjunction with three distinct ML algorithms: Support Vector Machine (SVM), Deep Neural Net (DNN) and Random Forest (RF) to separate the liver and cancer more successfully from CT images. Discontinuities or variances in the GF-generated surface data between various slices of the same organ shouldn't exist. Initially, features are extracted at the pixel level using a variety of Gabor filters. The liver is then removed from an abdominal CT picture using three different classifiers, which is the second step in the liver segmentation process. Segmentation classifiers of tumor are then applied to the segmented liver image. The Gabor filter provides better representation to the human visual system (HVS) of perception, and all of the aforementioned classification algorithms have been effectively employed for pixel-wise segmentation issues [20]. In order to shorten the time and effort needed to diagnose liver cancer, Ayalew, Y.A., applied a deep learning approach to separate the liver and tumor from the images of stomach CT scan. The fundamental UNet design forms the basis of the algorithm. In this study, dropout layer and batch normalization were added after each block along the shrinking path, and the number of filters utilized in each block was decreased. The programme received dice scores of 0.96 for the division of the liver, 0.63 for the division of the tumors in the abdominal CT scan image and 0.74 for the segmentation of the liver tumor. The findings for the liver improved by 0.11 percentage and the results for the entire liver segmentation increased by 0.01 [21].

Rela, M. uses a unique approach for identifying liver cancers more effectively. Benchmark and manually collected datasets are processed using filtering and histogram equalization. Adaptive thresholding and level set segmentation are also used in this research to segment the liver. An upgraded deep learning technique called U-Net is used to segment the cancer using a novel Grey algorithm after the liver has been divided into segments. Since network training becomes increasingly difficult as feature length increases, the GW-CTO algorithm employs a multi-objective function. A Neural Network is subjected to the GW-CTO algorithm in order to further enhance these carefully selected features. The DNN outperformed PSO-HI-DNN, O-SHO-HI-DNN, CTO-HI-DNN, and GWO-HI-DNN by 2.4%, 5.2%, 4.3%, and 4.3%, respectively, while learning at an rate of 85% and with 4.3% accuracy [22]. To increase the efficiency of the clinical analysis, the author developed a novel method. The researchers planned to use fix-based CNN to predict class (normal or tumour) on patches taken from 60 liver tumor full side images [23]. The author's unique three-dimensional (3-D) CNN was proposed for tissue classification in medical imaging and used to distinguish between primary and metastatic liver cancers using scatter weighted MRI data. The suggested network consists of a fully associated layer with 2048 neurons, followed by a Softmax layer for twofold order, and four successive stride 3-D convolution layers with 3 × 3 × 3 bit size and redressed direct unit (ReLU) as actuation function [24].

According to earlier ML studies, for non-cancer patients, COVID-19 results can be predicted with outstanding accuracy using just a few clinical characteristics. For instance, Yan et al. claim that 90%+ performance may be achieved with just three parameters (C-reactive protein, absolute lymphocyte count and lactate dehydrogenase) [25]. Absolute neutrophil count, prothrombin time, absolute lymphocyte count, White blood cell count, D-dimer, albumin, procalcitonin total bilirubin, troponin I and lactate dehydrogenase are the 10 clinical variables for which Huang et al. showed statistical significance. Many of the clinical characteristics utilized in this study were also included in other investigations [26]. Yan et al. and Huang et al utilized dataset variables to trained two random forest classifiers, for a fair comparison and to evaluate if variables previously deemed as relevant could also well-predict outcomes for cancer patients.

3. Research Methodology

This experimental research has recognized and concentrated on DL models that assist in determining high accuracy in performance of liver cancer detection even during COVID-19 situations. The proposed LSTM model that is one of the most suitable model for sequential data to identify liver cancer even if the patients are affected with COVID-19 the extracted features. In general, the LSTM model assist in initiating dense layer by modifying the activation function of input. This activation functions help in recognizing the sequential pattern of input data during feature extraction has generated better understanding of data. Therefore, LSTM model has memory cells that can able to remember the data for long time span. The architecture of sequential pattern of LSTM to detect liver cancer during COVID-19 is shown in figure 1.

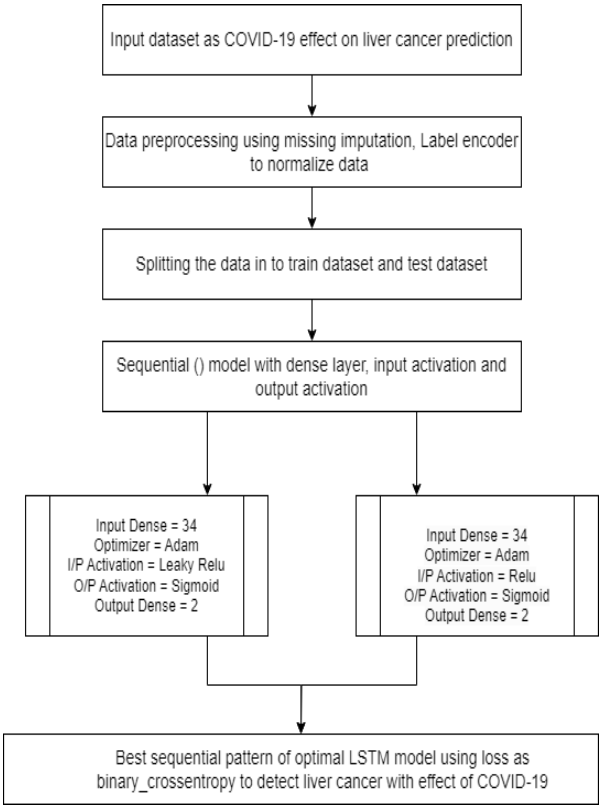

Figure 1: Architecture for sequence based LSTM for live cancer detection at COVID-19

3.1 Dataset collections and preprocessing

The dataset is involved with details of COVID-19 effected patients with LC that yet to be confirmed but these European data has been reported with disruption to Hepatocellular Carcinoma (HCC) services. During the first wave of the pandemic from Feburary 2020 to May 2020, the reduction in incident cases and impact on management. The data is generally collect from all patients mentioned to the Newcastle Upon Tyne (NUTH) foundation trust within first year of the pandemic from March 2020 to February 2021has been compared with retrospective observational cohort of ensuing the patients presented in the 12 months are immediately preceding it is shown in figure 2. The recent cases are HCC diagnosis are confirmed through histological or radiological test based on the procedure of COVID-19.

Cancer	Year	Month	Bleed	Mode_Presentation	Age	Gender	Etiology	Cirrhosis	Size
Y	Prepande	1	N	Surveillance	68	M	NAFLD	Y	2
Y	Prepande	1	N	Surveillance	70	M	ARLD	Y	4
Y	Prepande	1	N	Surveillance	64	M	ARLD	Y	5
Y	Prepande	1	N	Incidental	73	M	ARLD	Y	8
Y	Prepande	1	N	Incidental	66	F	ARLD	Y	6
Y	Prepande	1	N	Incidental	70	M	NAFLD	Y	2
Y	Prepande	1	N	Incidental	73	M	NAFLD	Y	2
Y	Prepande	1	N	Incidental	67	M	NAFLD	N	4
Y	Prepande	1	N	Surveillance	57	M	HCV	Y	3
Y	Prepande	1	N	Incidental	75	M	NAFLD	Y	8
Y	Prepande	1	N	Incidental	81	F	No establ	N	10
Y	Prepande	1	N	Surveillance	82	M	NAFLD	N	2
Y	Prepande	1	N	Surveillance	74	M	NAFLD	Y	1
Y	Prepande	1	N	Incidental	76	M	NAFLD	N	15
Y	Prepande	2	N	Surveillance	66	M	ARLD	Y	2
Y	Prepande	2	N	Incidental	78	F	NAFLD	N	4
Y	Prepande	2	N	Surveillance	82	F	PBC/AIH	Y	1
Y	Prepande	2	N	Symptomatic	71	F	ARLD	Y	5
Y	Prepande	2	N	Symptomatic	66	M	NAFLD	N	11
Y	Prepande	2	N	Incidental	73	M	NAFLD	Y	1
Y	Prepande	2	N	Incidental	86	M	NAFLD	Y	5
Y	Prepande	2	N	Surveillance	77	M	ARLD	Y	1
Y	Prepande	2	N	Surveillance	57	M	ARLD	Y	3
N	Prepande	2	NA	Surveillance	64	F	PBC/AIH	Y	2

Figure 2: Sample of LC prediction on COVID-19 effect dataset.

Sl.No	Attribute Name	Attribute description
1	Cancer	Flag of the cancer status as [Y/N]
2	Year	Prepandemic or Postpandemic
3	Month	Month of the year from 1 to 12
4	Bleed	Status of bleeding as [Y/N]
5	Mode Presentation	Presentatin mode as Symptomatic/incidental/ Surveillence
6	Age	Patients age
7	Gender	Male (M)/Female (F)
8	Etiology	No established CLD, ARLD, NAFLD, HCV, HH, PBC/AIH and HBV
9	Cirrhosis	Patients under liver disease or not [Y/N]
10	Size	Diameter of Tumour in mm
11	HCC TNM Stage	Hepatocellular carcinoma Tumour node metastasis Stage ("I", "II", "IIIA+IIIB", "IV")
12	HCC BCLC Stage	Hepatocellular carcinoma Barcelona Clinic for Liver Cancer Stage ("0", "A", "B", "C", "D")
13	ICC TNM Stage	Intrahepatic cholangiocarcinoma
		Tumour node metastasis Stage ("I", "II", "III", "IV")
14	Treatment grps	Ablation, Supportive care, TACE, SIRT, Medical and OLTx
15	Survival from MDM	Survival from Multidisciplinary meeting
16	Alive Dead	Status of patients as "Alive" or "Dead"
17	Type of incidental finding	Primary care-routine, Secondary care-routine, Primary care-acute or Secondary care-acute
18	Surveillance programme	Patient in a formal surveillance programme ("Y", "N")

Table 1: Attributes in LC prediction on covid-19 effect dataset

There are 450 cases on the first year of pandemic is identified which can be measured and defined with the feature of about 18 columns is shown in Table 1. The dataset features are correlate with each features and plotted is shown in figure 3.

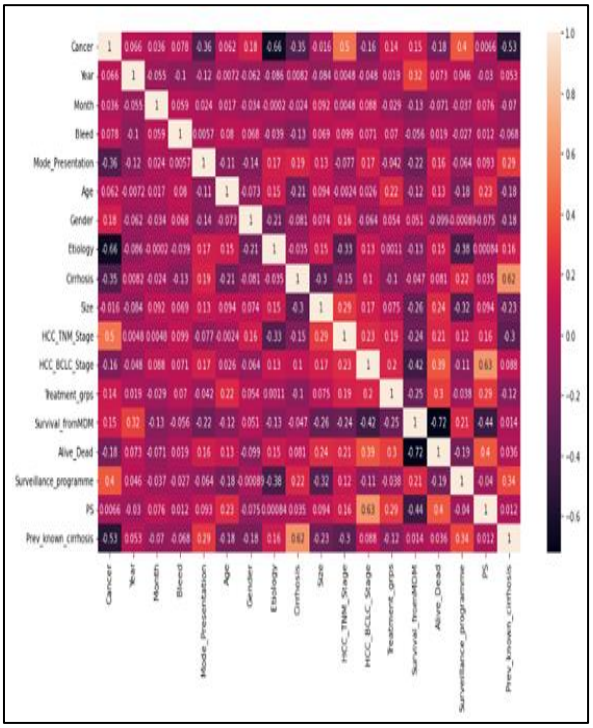

Figure 3: Correlation heat map for Liver cancer on COVID-19

3.2 Feature Extraction

The LSTM model with sequential kernel has imported for better input analysis using 34 unit of input data using 17 features in which input

activation is involved with Relu function and Leaky Relu function. The output dense layer used is 2 whereas the activation function is sigmoid and the optimizer used is adam. The length of the words also calculated for the entire dataset articles and maximum review length is kept as 100 for threshold in this research which may reduce the execution time of the model. The dataset get split with 70% of the article as train dataset and 30% is used in testing purposes.

3.3Working of LSTM model

The LSTM consists of only one unit namely LSTM unit which involve four Feed Forward Neural Network (FFNN). Every NN contain both input as well as output layer. In every NN, the input as well as output layer is involved whereas input neurons get connected to all output neurons. Thus, the resulted LSTM unit consists of four fully connected layers. The general LSTM node structure working is available in figure 4. This structure of LSTM involves three different gate such as input gate (i), forgot gate (f) as well as output gate (o) correspondingly. Let consider memory cell (c) and new memory cell (g) correspondingly. Based on these operations, the LSTM model can assist in controlling the data flow between hidden nodes and the preceding hidden output for the suitable periods in generating the recent output. Identify the memory cell and the new memory cell as c and g respectively. Using these procedures, it is possible to manage the data flow between hidden nodes and choose the prior hidden outputs at the right moments to produce the present result. Especially for the preceding hidden output h_t and the present input X_{t+1}, the present hidden output h_{t+1} has been calculated through equation 1 – 6.

$$i_{t+1} = \sigma\left(U^{[i]}.X_{t+1} + W^{[i]}.h_t\right) \quad (1)$$

$$o_{t+1} = \sigma\left(U^{[o]}.X_{t+1} + W^{[o]}.h_t\right) \quad (2)$$

$$f_{t+1} = \sigma\left(U^{[f]}.X_{t+1} + W^{[f]}.h_t\right) \quad (3)$$

$$g_{t+1} = tanh\left(U^{[g]}.X_{t+1} + W^{[g]}.h_t\right) \quad (4)$$

$$h_{t+1} = tanh(c_{t+1}) \odot i_{t+1} \quad (5)$$

$$c_{t+1} = c_t \odot f_{t+1} + g_{t+1} \odot i_{t+1} \quad (6)$$

Where,

$\odot$ = Hadamard product

σ = Logistic sigmoid function

$U^{[\alpha]}$ and $W^{[\alpha]}$ = weight matrix for current input and previous hidden output

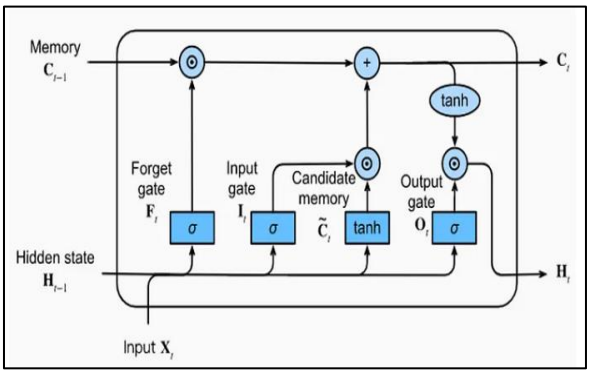

Figure 4: LSTM structure in RNN model

There is certain research suggesting that the performance of LSTM technique is better than conventional RNNs in numerous real-world scenarios which have significantly greater parameters than a conventional RNN with a similar size. When the assignment data is not high-dimensional, the outcome is more probable to make training harder also leading to over fitting. A few can create a different type of RNN by emerging certain gates in the hidden layer to overwhelm this limitation.

3.4 Algorithm for embedded layer RNN model

Step 1: Load the collect data of first year pandemic COVID-19 with LC patients.

Step 2: Data preprocessing by missing imputation and label encoder for identifying the sentiments.

Step 3: Length of the entire dataset words are calculated and kept maximum threshold assigned for total review length is 100.

Step 4: Data get split into train and test dataset to build LSTM with various input activation function as Relu and Leaky Relu as well as Adam as an optimizer and subsequent layers for hidden and output layers.

Step 5: The accuracy for validation metrics monitored by fitting the model to the 'X_train' and 'y_train' data.

Result And Discussion

Python 3.9.0 is used to implement the DL model, and several libraries included keras, matplot and sklearn are used. The experimental setup is prepared in accordance with the features of the

dataset. The dataset get split into 70% train dataset as well as 30% test dataset in which 315 cases are considered for train. The matrix of word embedding has been pretrained with respect to an entire text corpus in LSTM model. The activation function is significant in classifying the sequence pattern and the pattern is applied to both LSTM and GRU model which is evaluated by test cases using 135 cases and the accuracy for 100 epochs is illustrated in figure 5 and evaluated through confusion matrix class value. The last 19 epochs are illustrated with accuracy and loss for train and test.

Figure 6 illustrated the accuracy of the LSTM model with leaky relu as activation function whereas the fluctuation in data is identified from 0.0 epoch to 100 epoch with an accuracy score as 0.568 to 0.981 for train dataset. In the case of test dataset, the accuracy have shifted from 0.568 to 0.674 and end till 0.993 for epoch 0 to 100. Due to better understanding in the train dataset, the model with leaky relu show enhanced test accuracy.

```
Epoch 81/100
32/32 [==============================] - 0s 4ms/step - loss: 0.0628 - accuracy: 0.9714 - val_loss: 0.0481 - val_accuracy: 0.9704
Epoch 82/100
32/32 [==============================] - 0s 3ms/step - loss: 0.0644 - accuracy: 0.9714 - val_loss: 0.0334 - val_accuracy: 0.9852
Epoch 83/100
32/32 [==============================] - 0s 4ms/step - loss: 0.0359 - accuracy: 0.9873 - val_loss: 0.0343 - val_accuracy: 0.9852
Epoch 84/100
32/32 [==============================] - 0s 3ms/step - loss: 0.0504 - accuracy: 0.9746 - val_loss: 0.0356 - val_accuracy: 0.9852
Epoch 85/100
32/32 [==============================] - 0s 4ms/step - loss: 0.0688 - accuracy: 0.9714 - val_loss: 0.0320 - val_accuracy: 0.9852
Epoch 86/100
32/32 [==============================] - 0s 3ms/step - loss: 0.0552 - accuracy: 0.9810 - val_loss: 0.0425 - val_accuracy: 0.9778
Epoch 87/100
32/32 [==============================] - 0s 4ms/step - loss: 0.0610 - accuracy: 0.9778 - val_loss: 0.0421 - val_accuracy: 0.9778
Epoch 88/100
32/32 [==============================] - 0s 3ms/step - loss: 0.0329 - accuracy: 0.9937 - val_loss: 0.0279 - val_accuracy: 0.9852
Epoch 89/100
32/32 [==============================] - 0s 3ms/step - loss: 0.0477 - accuracy: 0.9841 - val_loss: 0.0426 - val_accuracy: 0.9852
Epoch 90/100
32/32 [==============================] - 0s 4ms/step - loss: 0.0566 - accuracy: 0.9810 - val_loss: 0.0725 - val_accuracy: 0.9630
Epoch 91/100
32/32 [==============================] - 0s 3ms/step - loss: 0.0530 - accuracy: 0.9810 - val_loss: 0.0248 - val_accuracy: 0.9926
Epoch 92/100
32/32 [==============================] - 0s 3ms/step - loss: 0.0533 - accuracy: 0.9778 - val_loss: 0.0428 - val_accuracy: 0.9778
Epoch 93/100
32/32 [==============================] - 0s 3ms/step - loss: 0.0358 - accuracy: 0.9810 - val_loss: 0.0265 - val_accuracy: 0.9852
Epoch 94/100
32/32 [==============================] - 0s 4ms/step - loss: 0.0391 - accuracy: 0.9841 - val_loss: 0.0378 - val_accuracy: 0.9852
Epoch 95/100
32/32 [==============================] - 0s 4ms/step - loss: 0.0630 - accuracy: 0.9683 - val_loss: 0.0406 - val_accuracy: 0.9852
Epoch 96/100
32/32 [==============================] - 0s 3ms/step - loss: 0.0607 - accuracy: 0.9746 - val_loss: 0.0372 - val_accuracy: 0.9852
Epoch 97/100
32/32 [==============================] - 0s 3ms/step - loss: 0.0272 - accuracy: 0.9937 - val_loss: 0.0264 - val_accuracy: 0.9852
Epoch 98/100
32/32 [==============================] - 0s 4ms/step - loss: 0.0413 - accuracy: 0.9778 - val_loss: 0.0353 - val_accuracy: 0.9852
Epoch 99/100
32/32 [==============================] - 0s 4ms/step - loss: 0.0281 - accuracy: 0.9905 - val_loss: 0.0394 - val_accuracy: 0.9852
Epoch 100/100
32/32 [==============================] - 0s 4ms/step - loss: 0.0454 - accuracy: 0.9810 - val_loss: 0.0303 - val_accuracy: 0.9926
```

Figure 5: Sequential pattern with leaky relu activation function for LSTM model

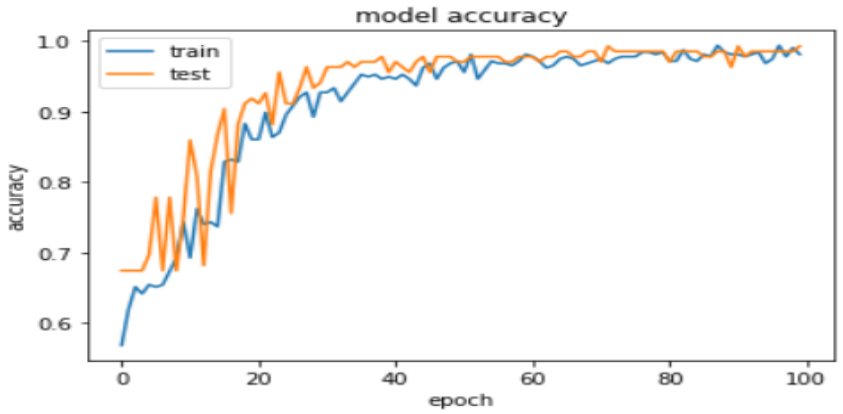

Figure 6: Model accuracy for LSTM model

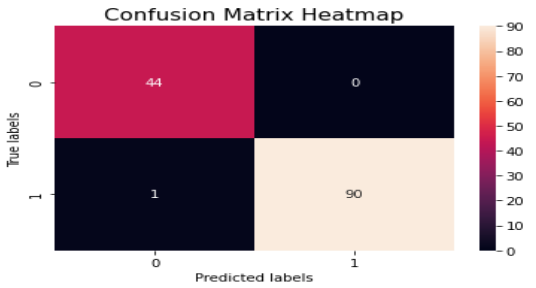

Figure 7: LSTM model Confusion matrix

Figure 7 illustrates the possibility amount for four different classes which shows that True positive (TP) represent the correctly predicted LC with COVID-19 and True negative (TN) represent correctly predicted No LC but COVID-19. The False Positive (FP) represent the actual LC with COVID-19 as not a LC with COVID-19 and similarly False Negative (FN) represent the No LC but COVID-19 but consider as LC with COVID-19 shown in table 2.

Table 2: Confusion matric classes for LC prediction on covid-19 effect

Classification Model	Confusion Matrix for the fake news detection			
	TP	TN	FP	FN
LSTM with Leaky Relu	90	44	0	1
LSTM with Relu	91	42	2	0

Table 3: Evaluation metrics for classification model

Classification model	Accuracy (%)	Precision (%)	Recall (%)	F1-Score (%)	Sensitivity	Specificity
LSTM with Leaky Relu	**99.26**	**99.98**	**98.9**	**99.44**	**0.989**	**0.999**
LSTM with Relu	**98.52**	**97.85**	**99.98**	**98.91**	**0.999**	**0.954**

Table 3 illustrates the evaluation metrics for LSTM based sequential pattern model with activation function with Leaky Relu model and with activation function with Relu model. The accuracy, precision shows the true positive rate with LSTM of sequential activation function as Leaky Relu and relu function model. The true positive rate and true negative rate can be determined through sensitivity and specificity values of evaluation metrics of diagnosis of LC patients during COVID-19.

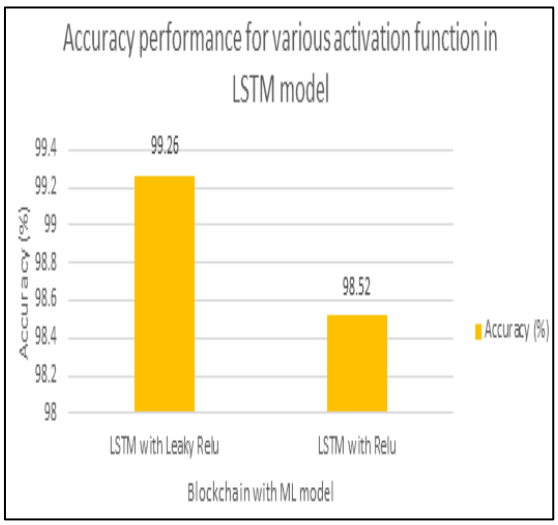

Figure 8: Accuracy for various RNN model

Figure 8 has illustrates the accuracy of the proposed sequence based LSTM with leaky relu is 99.26% has better efficiency in prediction fake news while compared to sequence based LSTM with relu method is 98.52%. This shows the sequential based LSTM with leaky relu model has better understanding of detecting LC during COVID-19 with high accuracy.

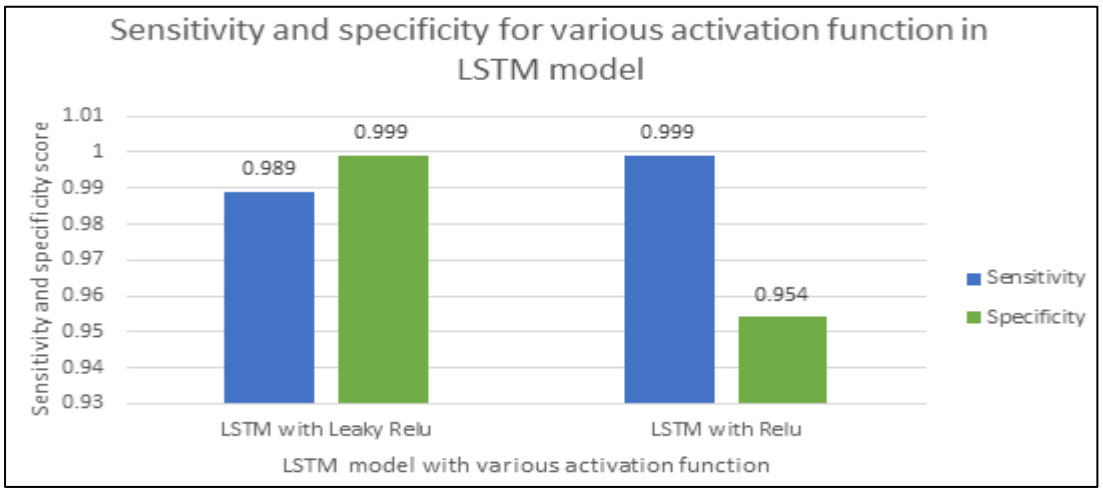

Figure 9: Sensitivity and Specificity of fake news detection

Figure 9 illustrates the sensitivity and specificity of proposed LSTM sequence based activation function leaky relu and relu models in which both model contribute better in one and other evaluation metrics. In the case of Specificity, the leaky relu function sequential based LSTM model has better score as 0.999 compared to LSTM with relu model is 0.954 respectively. Likewise, the sensitivity of LC during COVID-19 classification has high true negative rate with relu sequence based LSTM model with 0.999 which is high while compare to leaky relu function of LSTM model is 0.989 correspondingly.

Conclusion

The most challenging area in healthcare data mining with COVID-19 because of availability of structured data and unstructured data. There are certain procedure to be followed in predicting COVID-19 diagnosis as per WHO norms. These kind of norm is also complex for the certain patients like cancer and cardiac disease patients in which LC is one of the complex cancer and recovered

COVID-19 through vaccination and medicine that are not available during that situation. Hence, it is essential for managing patients under quarantine at home or a facility. Moreover, it is critical in LC patients with COVID-19 on the infection severity basis for securing the complete medical system of the world. Thus, several models have been developed to predict the prognosis of patients with confirmed COVID-19 or the possibility of COVID-19 diagnosis of patients before confirmation. The DL method involved in detecting the LC with high precision and accuracy in which LSTM may support due to Long period memory. Based on the activation function with various sequence pattern in the LSTM model is recognized individually and generate with high accuracy result is considered to be best LSTM sequential model. The leaky relu sequential pattern in LSTM is considered to be best model in predicting LC patient even during COVID-19 exactly. The evaluation of the LSTMs model is done by accuracy as well as sensitivity and specificity score which has been examined for both activation functions sequential-based LSTM. This performance leads us to the conclusion that the proposed leaky relu sequential-based LSTM performs better than relu sequential-based LSTM with highly accurate in classifying LC during COVID-19.

References

[1]. Sumedh Sontakke,Jay Lohokare, Reshul Dani3, Department of Computer and IT, Department of Electrical Engineering College of Engineering, Pune ,"Diagnosis of Liver Diseases using Machine Learning ", 2017 International Conference on Emerging Trends & Innovation in ICT (ICEI) Pune Institute of Computer Technology, Pune, India, Feb 3-5, 2017.

[2]. Aman Singh; Babita Pandey,"An Euclidean Distance based KNNComputational Method for Assessing Degree of Liver Damage",2016 International Conference on Inventive Computation Technologies (ICICT),7823222, 2016 IEEE.

[3]. Kiani, A.; Uyumazturk, B.; Rajpurkar, P.; Wang, A.; Gao, R.; Jones, E.; Yu, Y.; Langlotz, C.P.; Ball, R.L.; Montine, T.J.; et al. Impact of a deep learning assistant on the histopathologic classification of liver cancer. NPJ Digit. Med. 2020, 3, 23. [CrossRef] [PubMed]

[4]. Chennam, K.K.; Uma Maheshwari, V.; Aluvalu, R. Maintaining IoT Healthcare Records Using Cloud Storage. In IoT and IoE Driven Smart Cities; Springer: Cham, Switzerland, 2022; pp. 215–233.

[5]. Ali L, Wajahat I, Golilarz NA, Keshtkar F, Bukhari SAC. LDA-GA-SVM: improved hepatocellular carcinoma prediction through dimensionality reduction and genetically optimized support vector machine. Neural Comput Appl. 2021;33(7):2783–92.

[6]. Li HM. Microcirculation of liver cancer, microenvironment of liver regeneration, and the strategy of Chinese medicine. Chin J Integr Med. 2016;22(3):163–7.

[7]. Bray F, Ferlay J, Soerjomataram I, Siegel RL, Torre LA, Jemal A. Global cancer statistics 2018: GLOBOCAN estimates of incidence and mortality worldwide for 36 cancers in 185 countries. CA-Cancer J Clin. 2018;68(6):394–424.

[8]. Liao HT, Xiong TY, Peng JJ, Xu L, Liao MH, Zhang Z, Wu ZR, Yuan KF, Zeng Y. Classifcation and prognosis prediction from histopathological images of hepatocellular carcinoma by a fully automated pipeline based on machine learning. Ann Surg Oncol. 2020;27(7):2359–69.

[9]. Sun CF, Wang YX, Sun MY, Zou Y, Zhang CC, Cheng SS, Hu WP. Facile and cost-efective liver cancer diagnosis by water-gated organic feld-efect transistors. Biosens Bioelectron. 2020;164:6.

[10]. Eslam M, Newsome PN, Sarin SK, Anstee QM, Targher G, Romero-Gomez M et al (2020) A new defnition for metabolic dysfunction-associated fatty liver disease: an international expert consensus statement. J Hepatol 73(1):202–209.

[11]. Ji D, Qin E, Xu J, Zhang D, Cheng G, Wang Y et al (2020) Non-alcoholic fatty liver diseases in patients with COVID-19: a retrospective study. J Hepatol 73(2):451–453

[12]. Tripon S, Bilbault P, Fabacher T, Lefebvre N, Lescuyer S, Andres E et al (2022) Abnormal

liver tests and non-alcoholic fatty liver disease predict disease progression and outcome of patients with Covid-19. Clin Res Hepatol Gastroenterol 25:101894.

[13]. Meijnikman AS, Bruin S, Groen AK, Nieuwdorp M, Herrema H (2021) Increased expression of key SARS-CoV-2 entry points in multiple tissues in individuals with NAFLD. J Hepatol 74:748– 760.

[14]. Muñoz-Martínez, S., Sapena, V., Forner, A., Nault, J.-C., Sapisochin, G., Rimassa, L., … Hołówko, W. (2021). Assessing the impact of COVID-19 on liver cancer management (CERO-19). JHEP Reports, 3(3), 100260.

[15]. Afza F, Sharif M, Khan MA, Tariq U, Yong H-S, Cha J. Multiclass skin lesion classifcation using hybrid deep features selection and extreme learning machine. Sensors. 2022;22(3):799.

[16]. Lin, H., Wei, C., Wang, G., Chen, H., Lin, L., Ni, M., … Zhuo, S. (2019). Automated classification of hepatocellular carcinoma differentiation using multiphoton microscopy and deep learning. Journal of Biophotonics, e201800435.

[17]. Coudray, N. et al. Classification and mutation prediction from non-small cell lung cancer histopathology images using deep learning. Nat. Med. 24, 1559–1567 (2018).

[18]. Skrede, O. J. et al. Deep learning for prediction of colorectal cancer outcome: a discovery and validation study. Lancet 395, 350–360 (2020).

[19]. Bera, K., Schalper, K. A., Rimm, D. L., Velcheti, V. & Madabhushi, A. Artificial intelligence in digital pathology—new tools for diagnosis and precision oncology. Nat. Rev. Clin. Oncol. 16, 703–715 (2019).

[20]. Ashreetha, B.; Devi, M.R.; Kumar, U.P.; Mani, M.K.; Sahu, D.N.; Reddy, P.C.S. Soft optimization techniques for automatic liver cancer detection in abdominal liver images. Int. J. Health Sci. 2022, 6, 10820–10831.

[21]. Ayalew, Y.A.; Fante, K.A.; Mohammed, M.A. Modified U-Net for liver cancer segmentation from computed tomography images with a new class balancing method. BMC Biomed. Eng. 2021, 3, 4.

[22]. Rela, M.; Suryakari, N.R.; Patil, R.R. A diagnosis system by U-net and deep neural network enabled with optimal feature selection for liver tumor detection using CT images. Multimed. Tools Appl. 2022, 82, 3185–3227.

[23]. Wang, J., Xu, Z., Pang, ZF. et al.Tumour detection for whole slide image of liver based on patch-based convolutional neural network. Multimed Tools Appl (2020). https://doi.org/10.1007/s11042- 020-09282-x.

[24]. E. Trivizakiset al., "Extending 2-D Convolutional Neural Networks to 3-D for Advancing Deep Learning Cancer Classification With Application to MRI Liver Tumour Differentiation," in IEEE Journal of Biomedical and Health Informatics, vol. 23, no. 3, pp. 923-930, May 2019, doi: 10.1109/JBHI.2018.2886276.

[25]. Yan L, Zhang H-T, Goncalves J, Xiao Y, Wang M, Guo Y, et al. An interpretable mortality prediction model for COVID-19 patients. Nat Mach Intell. 2020;2: 283–288.

[26]. Guan W-J, Ni Z-Y, Hu Y, Liang W-H, Ou C-Q, He J-X, et al. Clinical Characteristics of Coronavirus Disease 2019 in China. N Engl J Med. 2020;382: 1708–1720.